Spectral Analysis of Topological Defects in an Artificial Spin-Ice Lattice

Sebastian Gliga, Attila Kákay, Riccardo Hertel, and Olle G. Heinonen

Spectral analysis of topological defects in an artificial spin-ice lattice

Sebastian Gliga,[1,] [*] Attila Kákay,[2] Riccardo Hertel,[3] and Olle G. Heinonen[4, 5]

[1] *Center for Nanoscale Materials, Argonne National Laboratory, Lemont, IL 60439, USA*
[2] *Peter Grünberg Institute, Forschungszentrum Jülich, 52425 Germany*
[3] *IPCMS UMR7504, CNRS and UdS, Strasbourg, France*
[4] *Materials Science Division, Argonne National Laboratory, Lemont, IL 60439, USA*
[5] *Department of Physics and Astronomy, Northwestern University, 2145 Sheridan Rd., Evanston, IL 60208-3112*

Arrays of suitably patterned and arranged magnetic elements may display artificial spin-ice structures with topological defects in the magnetization, such as Dirac monopoles and Dirac strings. It is known that these defects strongly influence the quasi-static and equilibrium behavior of the spin-ice lattice. Here we study the eigenmode dynamics of such defects in a square lattice consisting of stadium-like thin film elements using micromagnetic simulations. We find that the topological defects display distinct signatures in the mode spectrum, providing a means to qualitatively and quantitatively analyze monopoles and strings which can be measured experimentally.

Spin ices are magnetic structures in which the interactions lead to frustration resulting in complex magnetic ordering and collective behavior [1–3]. *Artificial* spin-ice lattices are patterned nanoscale structures in which each element is small enough to have essentially uniform magnetization. The geometrical arrangement of the structures in the lattice leads to frustration by design. Examples of artificial spin ice are the Kagome lattice [4] and the stadium square lattice, consisting of stadium-shaped elements on a square lattice [5–7]. The equilibrium configuration and magnetization reversal of such lattices have been the subject of intense study [8–11]. Topological defects, in which the magnetization at a vertex is in a one-in-three-out (or three-in-one-out) configuration [12] have been observed in square lattices [5] and in Kagome lattices [13]. Such defects are similar to Dirac monopoles [14] and typically occur in pairs (*e.g.* monopole-antimonopole) connected by a defect string, or "Dirac string", along which the magnetization is reversed with respect to a lattice reference state. Dirac strings have been observed in Kagome lattices [15] and square lattices [10]. (Fig. 1). Recent studies have shown that these defects profoundly affect the equilibrium behavior and the magnetization reversal of such lattices [8, 10, 11, 16–19]. An interesting, yet unexplored question is whether the presence of such defects affects the resonant dynamics of the spin-ice lattice. Here, we investigate the frequency spectrum of eigenmodes, or resonances, of topological defects in a square spin ice lattice using micromagnetic simulations. We show that each topological defect displays distinct and localized features, both spatially as well as in frequency. These features act as a fingerprint for the type of defect and moreover allow to quantify the number of defects present in the lattice. We also show how spectral features in a lattice arise from the magnetostatic coupling between the edge-like modes of isolated elements. The coupling leads to multiplets that are split depending on the local magnetization configuration. In addition, the fundamental uniform mode of a single stadium is split in the presence of topological
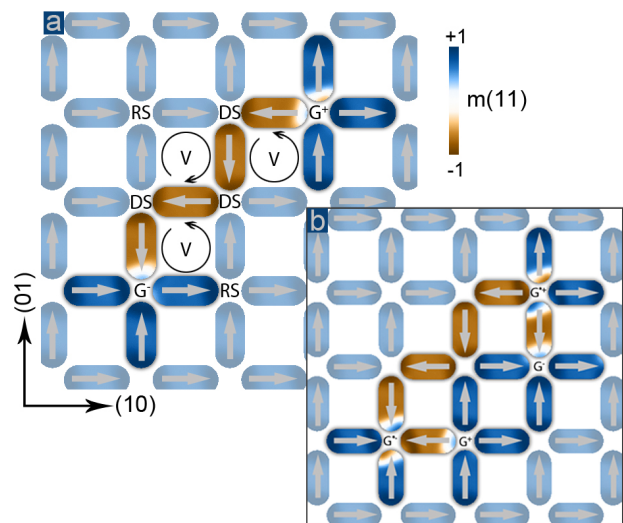
Figure 1. (Color online) a) Simulated singly-charged monopole pair (G^+G^-) linked by a Dirac string (DS). Vortices V form along the string. The reference state (RS) of the lattice is shown in pale blue, while the string and monopoles are highlighted. b) Doubly-charged monopoles can also be observed experimentally, although relatively rarely [5]. In this case, each vertex with a doubly-charged monopole leads to the formation of an adjacent oppositely-charged monopole (for example G^- forms next to a G^{*+} vertex). The colormap corresponds to the projection of the magnetization along the (11) direction of the string; the magnetic charge is taken as positive when the magnetization points out of the vertex.

defects.

We have studied the resonances of square spin ice lattices consisting of 112 Permalloy (Py) elements (Fig. 2a) with micromagnetic simulations using a fully three-dimensional finite-element algorithm based on the Landau-Lifshitz-Gilbert equation [20]. Each element (stadium) is 290 nm long, 130 nm wide, 20 nm thick and is discretized into about 22800 tetrahedral elements, corresponding to a cell size of about 3 nm^3. The lattice constant of the array is 390 nm. The material parameters
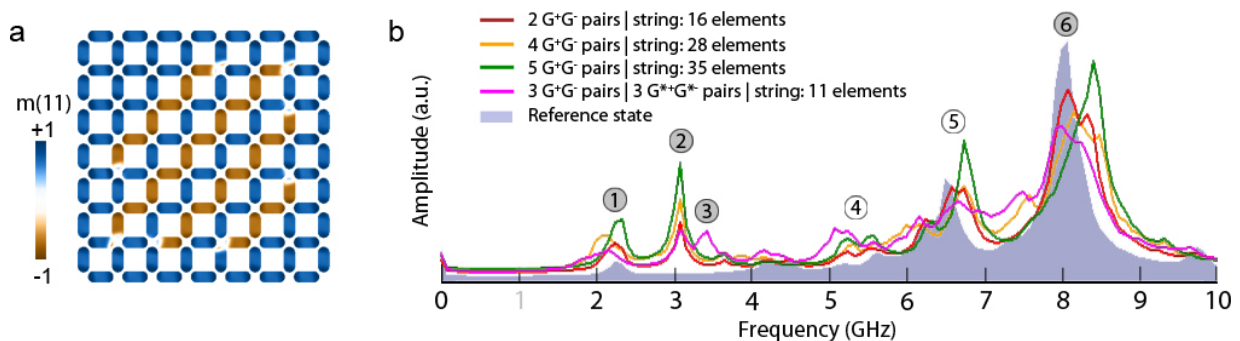
Figure 2. (Color online) (a) Simulated lattice composed of 112 magnetic elements. It contains four monopole-antimonopole pairs connected by Dirac strings extending over 28 elements. (b) Evolution of the magnetization dynamics spectrum with increasing string length and number of monopole-antimonopole pairs compared to the reference state. The shaded labels correspond to the main, distinct signatures of the topological defects. The amplitude units are identical in all cases.

chosen for Py are the following: $A = 13$ pJ/m (exchange constant), $\mu_0 M_s = 1.0$ T, and zero magnetocrystalline anisotropy [21]. We prepared a reference state (RS) of the lattice [22] by saturating the array along the (11) direction and adiabatically removing the external field (see Fig. 1). The system then relaxes into a state with the magnetization oriented along the $+y$ direction in the vertical elements and along the $+x$ direction for the horizontal elements of the array. We arbitrarily insert topological defects with charges ± 1 and ± 2 ($G^{\pm}$ and $G^{*\pm}$, respectively) connected by Dirac strings (DS) of variable length corresponding to typical observed configurations by reversing the magnetization in selected stadiums, and subsequently relaxing the magnetization (see Fig. 1). The dynamics and spectrum of eigenmodes of the lattice is then obtained by applying a short perturbation (5 mT field pulse in the (11) direction for 20 ps) and integrating the LLG equation in time.

The excitation spectrum of the RS is shown in Fig. 2(b) as the grey, filled area. It is characterized by a few prominent peaks corresponding to distinct eigenmodes. The first one (at position (1)), slightly above 2 GHz, corresponds to edge excitations of the outermost stadium elements at the boundary of the lattice. A weaker mode appears above 4 GHz corresponding to edge excitations of the magnetostatically coupled elements inside the lattice. Two modes, labeled (4), are visible slightly above 5 GHz, in which the elements on the boundary of the lattice display higher order edges modes that couple to modes on elements adjacent to the boundary elements. Above 6 GHz, label (5) indicates a mode corresponding to higher-order edge oscillations of the individual elements. This mode is split: owing to their smaller magnetostatic coupling, the elements at the boundary of the lattice oscillate at a slightly lower frequency than elements in the interior of the lattice. Finally, a mode at 8 GHz (position (6)) corresponds to the ferromagnetic resonance in which the oscillation is approximately uniform in the interior of the elements. The colored lines

in Fig. 2(b) depict the spectrum evolution as topological defects and Dirac strings are inserted into the lattice. Near mode (1) of the RS a new mode associated with oscillations of the G^+G^- pairs appears. The amplitude of this mode increases with the number of monopole-antimonopole pairs. Later, we show that this mode is close in frequency to the edge modes of the RS, but is spatially localized at the monopoles. Therefore, it can be distinguished from the edge modes either in the thermodynamic limit or by using detection techniques sensitive to the interior of the lattice [23]. Similarly, around 5 GHz, a new mode associated with doubly-charged monopoles unfolds alongside the RS mode at (4). Above 6 GHz, oscillations of the monopole-antimonopole pairs give rise to a new mode within the lattice (red curve in Fig. 2 at label (5)). When a large number of pairs is present, this mode becomes dominant (green curve). Finally, at (6) the ferromagnetic resonance peak is split and shifted in the presence of Dirac strings. In addition to the modifications in the GS spectrum, two new resonances are observed: mode (2) at 3 GHz corresponds to edge modes of elements in the interior of a Dirac string while mode (3) at 3.5 GHz is due to oscillations of doubly-charged monopoles.

We now investigate in detail the modes associated with the different topological defects. Figure 3a refers to the mode associated with a G^+G^- pair at position (1) in Fig. 2. The static magnetization configuration is indicated by the arrows in the first column. The color maps (columns two and three) depict the oscillations of the x and y components of the magnetization, respectively, which are clearly localized at the monopoles. A splitting in the frequency peak is associated with the G^+G^- resonance (graph, fourth column): Monopoles located on the boundary of the lattice (green curves) contribute to the amplitude of edge oscillations of the RS configuration, thereby increasing the amplitude of the RS mode (indicated in the figure) slightly above 2.2 GHz. Monopole

configurations in the interior of the lattice oscillate at a lower frequency, around 2.1 GHz in this case (maroon curves). The peak amplitude increases linearly with the number of monopole pairs in both cases as shown in the last column (simulations were carried-out for a maximum number of five pairs). It is therefore possible not only to identify the presence of monopoles in the lattice, but equally to *quantify* the number of pairs, given a reference point. Figure 3b refers to the oscillations of the stadiums in the Dirac string connecting a G^+G^- pair position ② in Fig. 2. The spectral amplitude of this peak increases linearly with the total number of vertices in the string (string length). Figure 3c (position ③ in Fig. 2) shows the oscillations of a doubly-charged monopole pair. Again, we note the linear relationship between the number of monopole pairs and the spectral amplitude of the mode. From this linear relationship, it can be concluded that the different strings and monopoles are decoupled from each other, even though they are rather closely packed (see Fig. 2a) [24]. Finally, Fig. 3d (position ⑥ in Fig. 2 illustrates the splitting of the ferromagnetic resonance (FMR) mode [25]. The spatial oscillations are shown here by projecting the magnetization along the (11) direction of the string, as in Fig. 1, in order to optimize the contrast. The two color maps correspond to spatial oscillations at the bulk FMR frequency of 8 GHz (second column) and at 8.3 GHz (third column), showing that the splitting stems from the Dirac string, which oscillates at a higher frequency. The peak amplitude of the mode at 8.3 GHz therefore increases with increasing string length at the expense of the FMR peak at 8 GHz, as shown in the amplitude plot (rightmost panel). Again, a slight splitting occurs when the strings terminate on elements on the boundary of the lattice (green curves) or on elements in the interior lattice (maroon curves) because of the difference in magnetostatic coupling at the string extremities.

The magnetostatic coupling at the vertices drives the spectral features of the monopoles and the Dirac strings, and the magnitude of this coupling depends on the lattice constant. The experimental observability of these features clearly depends on their robustness with respect to variations in the lattice constant. Figure 4 shows simulations with different lattice constants for a given configuration composed of one monopole-antimonopole pair linked by a string spanning six stadiums. For comparison, the spectrum of a single stadium with initial equilibrium magnetization along the long axis of the element is shown (full shaded graph). There are three main peaks below 10 GHz for the single stadium. The first peak at 1.4 GHz corresponds to two modes of even and odd symmetry in which the dynamical part of the magnetization is localized near the edges of the stadium. Similarly, the peak at 5.7 GHz corresponds to two degenerate higher-order edge modes (one even and one odd) with additional
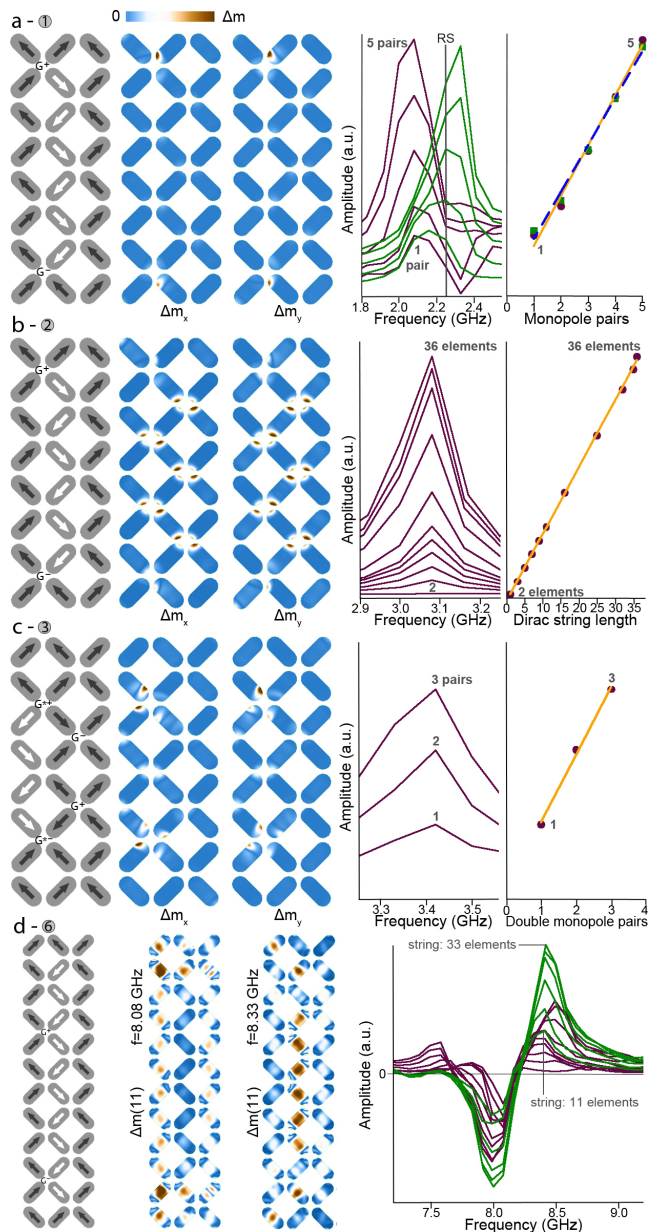
Figure 3. (Color online) Examples of local oscillations of the magnetization (Δm) characteristic for monopoles (a), Dirac strings (b) and doubly-charged monopoles (c). The first column shows the static magnetic configuration. The second and third columns respectively show the oscillations of the x and y components of the magnetization. The plots show the change in amplitude of the spectral signature of the different defects relative to the reference state. The last row (d) illustrates the splitting of the ferromagnetic resonance peak in the presence of a Dirac string. Labels are from Fig. 2.

nodal lines near the edges. Linear combinations of these edge modes couple magnetostatically in a lattice and give rise to multiplets, the splitting of which depends on the equilibrium structure of the magnetization at each vertex and on the lattice constant. Some of these linear combinations are localized near the vertices and are sensitive
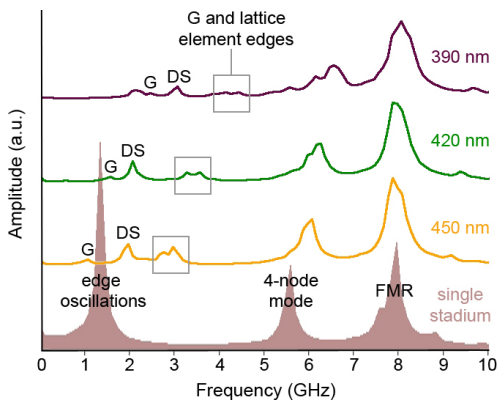
Figure 4. (Color online) Evolution of the spectral features with decreasing element separation for an array containing one monopole-antimonopole pair connected by a string of ten elements, compared to a single stadium. As the lattice constant of the array is reduced, the spectral features are redshifted while the amplitude of the ferromagnetic resonance peak decreases. *G*: peak characteristic of the monopole pair oscillations. *DS*: peak characteristic for the Dirac string oscillations.

to the local magnetization, and therefore to topological defects near the vertices. Finally, the peak at 8 GHz corresponds to the (bulk-like) uniform ferromagnetic resonance mode. In the presence of topological defects, with low magnetostatic coupling (lattice constant of 450 nm) the original peak at 1.4 GHz vanishes as the frequency of the edge oscillations is blue-shifted to 2.8 GHz (indicated by the square frame in the figure). Given that monopole modes are connected to oscillations of the element edges, a peak associated to the monopole pair also appears at 3 GHz. At lower frequencies (1 GHz), another distinct peak corresponds to oscillations of the monopole pair. This peak is blue-shifted when the lattice constant is decreased, and its frequency becomes comparable to the frequency of the edge excitation at elements on the lattice boundary at a spacing of 390 nm, as described earlier (Fig. 2 ①). An equally distinct peak corresponding to the Dirac string oscillation appears at 2 GHz for a 450 nm lattice constant and is red shifted. The higher order edge mode found in a single element (at 5.7 GHz) is robust: it persists for every lattice separation, eventually splitting as described earlier. As expected, the frequency of the ferromagnetic resonance mode remains unchanged. It is interesting to note that even for a lattice constant of 450 nm, the elements within a lattice remain sufficiently coupled to display features essentially different from the single stadium spectrum.

In summary, the presence and nature of topological defects display a one-to-one correspondence with the spectral features, which thus provide a means of experimentally identifying the presence of the different defects. The frequencies of the modes lie well within the range of experimental detection techniques such as a broadband me-

anderline approach [26], with an AC field provided by a microwave synthesizer and AC coils, or a pulsed field provided by a microwave stripline. Starting in the RS, applying a static reversal field with a magnitude close to the coercive field of the lattice should generate enough defects, Dirac monopoles and strings to provide sufficient signal to noise [11]. This would also allow for an estimation of the number of defects as the reversal field strength is varied past the coercive field. Moreover, the spectral amplitude of these features is proportional to the number of defects present, enabling a quantitative analysis based on the spectra. The appearance of localized modes at topological defects enables new possibilities of manipulating magnetization modes in spin-ice lattices, for example by inserting monopole pairs using spin polarized currents and propagating Dirac strings through the lattice. This may allow emerging applications combining magnonics, in which propagating spin waves in patterned magnetic thin films are manipulated, with artificial spin-ice lattices, in which localized spectral features based on topological defects can be tailored.

―――――

* Present address: Max-Planck-Institut für Mikrostrukturphysik, Weinberg 2, D-06120 Halle(Saale), Germany.

[1] D. J. P. Morris, D. A. Tennant, S. A. Grigera, K. B., C. C., R. Moessner, C. Czternasty, M. Meissner, K. C. Rule, J. U. Hoffmann, K. Kiefer, S. Gerischer, D. Slobinsky, and R. S. Perry, Science **326**, 5951 (2009).

[2] L. D. C. Jaubert and P. C. W. Holdsworth, Nature Physics **5**, 258 (2009).

[3] T. Fennell, P. P. Deen, A. R. Wildes, K. Schmalzl, D. Prabhakaran, A. T. Boothroyd, R. J. Aldus, D. F. McMorrow, and S. T. Bramwell, Science **326**, 415 (2009).

[4] Y. Qi, T. Brintlinger, and J. Cumings, Phys. Rev. B **77**, 094418 (2008).

[5] R. F. Wang, C. Nisoli, R. S. Freitas, J. Li, W. McConville, C. B. J., M. S. Lund, N. Samarth, C. Leighton, V. H. Crespi, and P. Schiffer, Nature **439**, 303 (2006).

[6] G. Möller and R. Moessner, Phys. Rev. Lett. **96**, 237202 (2006).

[7] A. Remhof, A. Schumann, A. Westphalen, H. Zabel, N. Mikuszeit, E. Y. Vedmdenko, T. Last, and U. Kunze, Phys. Rev. B **77**, 134409 (2008).

[8] J. Morgan, A. Stein, S. Langridge, and C. H. Marrows, Nature Physics **7**, 75 (2011).

[9] J. P. Morgan, A. Stein, S. Langridge, and C. H. Marrows, New J. Phys. **13**, 105002 (2011).

[10] C. Phatak, A. K. Petford-Long, O. Heinonen, M. Tanase, and M. De Graef, Phys. Rev. B **83**, 174431 (2011).

[11] C. Phatak, M. Pan, A. K. Petford-Long, S. Hong, and M. De Graef, New J. Phys. **14**, 075028 (2012).

[12] M. J. P. Gingras, Science **326**, 375 (2009).

[13] S. Ladak, D. E. Read, G. K. Perkins, L. F. Cohen, and

W. R. Branford, Nature Physics **6**, 359 (2010).

[14] P. A. M. Dirac, Proc. R. Soc. Lond. A **133** (1931).

[15] E. Mengotti, L. J. Heyderman, A. F. Rodriguez, F. Nolting, R. V. Hugli, and H. B. Braun, Nature Physics **7**, 68 (2011).

[16] A. Westphalen, A. Schumann, A. Remhof, H. Zabel, M. Karolak, B. Baxevanis, E. Y. Vedmedenko, T. Last, U. Kunze, and T. Eimueller, Phys. Rev. B **77**, 174407 (2008).

[17] V. Kapaklis, U. B. Arnalds, A. Harman-Clarke, E. T. Papaioannou, M. Karimipour, P. Kerelis, A. Taroni, P. C. W. Holdsworth, S. T. Bramwell, and B. Hjörvarsson, New J. Phys. **14**, 035009 (2012).

[18] Y. Shen, O. Petrova, P. Mellado, S. Dauenheimer, J. Cumings, and O. Tchernyshyov, New J. Phys. **14**, 035022 (2012).

[19] Z. Budrikis, K. L. Livesey, J. P. Morgan, J. Åkerman, A. Stein, S. Langridge, C. H. Marrows, and R. L. Stamps, New J. Phys. **14**, 035014 (2012).

[20] R. Hertel, S. Gliga, M. Fähnle, and C. M. Schneider, Phys. Rev. Lett. **98**, 117201 (2007).

[21] Similar results were also obtained using a fast Fourier transform method on a cubic lattice, with a mesh size of $\lesssim 1.25$ nm, in order to correctly account for the magnetostatic effects near the curved boundaries of the stadiums [R. E. Camley, *et al.*, Phys. Rev. B **78**, 024425 (2008)].

[22] L. A. Mól, R. L. Silva, R. C. Silva, A. R. Pereira, W. A. Moura-Melo, and B. V. Costa, Journal of Applied Physics **106**, 063913 (2009).

[23] For example, time-resolved Kerr microscopy. In a lattice of macroscopic dimensions, a meander transmission line can be placed near the interior of the lattice or patterned nano-elements such as magnetic tunnel junctions can be used to manipulate and detect local magnetization through the spin torque effect.

[24] When strings are adjacent to each other, they end in doubly-charged monopoles rather than singly-charged monopoles. Even then, however, we find that the strings are decoupled from each other. Stabilizing a doubly-charged monopole pair therefore either requires the presence of a singly-charged monopole-antimonopole pair (as shown in figure 2b) or of two strings.

[25] This peak actually corresponds to three near-degenerate distinct modes, two edge modes with two nodal lines (one odd and one even), and the bulk-like FMR mode.

[26] C. C. Tsai, J. Choi, S. Cho, S. J. Lee, B. K. Sarma, C. Thompson, O. Chernyashevskyy, I. Nevirkovets, and J. B. Ketterson, Review of Scientific Instruments **80**, 023904 (2009).